Int. J. Heat Mass Transfer. Vol. 17, pp. 1357–1364. Pergamon Press 1974. Printed in Great Britain

THE ONSET OF NATURAL CONVECTION AND ITS ENHANCEMENT OF HEAT TRANSFER IN STRATIFIED GAS–LIQUID FLOW

SCOTT C. HUNG and E. JAMES DAVIS
Department of Chemical Engineering, Clarkson College of Technology, Potsdam, N.Y. 13676, U.S.A.

(*Received* 28 *September* 1973 *and in revised form* 4 *February* 1974)

Abstract—The results of heat-transfer experiments and flow visualization studies are presented, showing the onset of natural convection in the liquid layer of a horizontal stratified gas–liquid flow heated from below by means of a step change in the wall heat flux. The Nusselt numbers, Nu, for combined free and forced convection are shown to be functions of the Rayleigh number, Ra_q, and the dimensionless axial distance, ξ. The data on the enhancement of heat transfer over that for the undisturbed flow (a Graetz problem) are well correlated by the dimensionless parameter $\phi = (Ra_q/Nu)^{1/4}/Nu_{Gz}$. The onset of natural convection occurs at $\phi = 2{\cdot}8$ for the narrow range of Prandtl numbers studied ($5 < Pr < 8$), which is in good agreement with an available theoretical analysis of the onset of natural convection in channels of rectangular cross-section.

NOMENCLATURE

A_n, Fourier coefficients in equation (15);
C_p, heat capacity [J/g°K];
E, local heat-transfer enhancement;
g, gravitational acceleration constant [cm/s^2];
J_m, Bessel functions;
k, thermal conductivity [J/cm s°K];
Nu, local Nusselt number, $q_w\delta/k(T_w - T_B)$ [dimensionless];
Nu_{Gz}, local Nusselt number, theoretical value for constant properties;
P, pressure [dyne/cm^2];
p, pressure [dimensionless];
Pr, local Prandtl number, $C_p\mu/k$ [dimensionless];
Pe, local Peclet number, $\overline{U}_m\delta/\alpha$ [dimensionless];
q_w, local wall heat flux [J/cm^2 s];
Ra_q, local Rayleigh number, $g\beta q_w\delta^4\rho^2C_p/k^2\mu$ [dimensionless];
Ra_T, local Rayleigh number, $g\beta(T_w - T_B)\delta^3\rho^2C_p/k\mu$ [dimensionless];
Re, local Reynolds number, $\overline{U}_m\delta/\nu$ [dimensionless];
T, temperature [°K];
T_0, inlet temperature [°K];
T_B, mixed mean liquid film temperature [°K];
T_w, wall temperature [°K];
U, V, W, axial, transverse, vertical velocity components [cm/s];
u, v, w, axial, transverse, vertical velocity components [dimensionless];
x, y, z, axial, transverse, vertical coordinates.

Greek symbols

α, thermal diffusivity [cm^2/s];
β, coefficient of thermal expansion [1/°K];
δ, liquid film thickness [cm];
∇^2, Laplace operator;
ζ, dimensionless vertical coordinate;
η, dimensionless transverse coordinate;
θ, dimensionless temperature, $(T - T_0)/(q_w\delta/k)$;
λ_n, eigenvalues;
μ, viscosity [g/cm s];
ν, kinematic viscosity [cm^2/s];
ξ, dimensionless axial coordinate;
ρ, density [g/cm^3];
σ, surface tension [dynes/cm];
ϕ, dimensionless parameter, $(Ra_q/Nu)^{1/4}/Nu_{Gz}$;
ψ_n, eigenfunction.

Subscripts

o, refers to the leading edge of the heated plate;
c, refers to the onset of the natural convection;
G, refers to the gas phase;
m, refers to the average value;
w, refers to the wall.

INTRODUCTION

TWO TYPES of instability can occur when a thin liquid film, heated from below, flows horizontally under the influence of a cocurrent gas stream (1) surface waves associated with momentum transfer from the gas phase and (2) natural convection due to energy transfer from

the heated boundary. If interfacial evaporation or non-uniform transfer of a chemical species between the phases produces surface tension variations, a third instability, Marangoni instability, is also possible.

These instabilities can significantly enhance heat transfer compared with that for stable smooth film flow. Frisk and Davis [1] measured the effects of wavy film flow in such two-phase systems, finding that when three-dimensional small amplitude waves and roll waves occur, heat transfer rates are increased by 100 per cent or more compared with smooth film flow under otherwise identical conditions. Two-dimensional ripples, however, provide no appreciable heat-transfer enhancement at the liquid–solid boundary.

When a hydrodynamically stable and initially isothermal liquid film passes over a surface with a step increase in wall temperature buoyant forces due to vertical density variations may destabilize the flow and induce heat-transfer enhancement by natural convection. Buoyancy effects are absent near the leading edge of the heated surface, but as the thermal boundary layer develops a point may be reached which the destabilizing buoyant force overcomes the stabilizing factors of viscosity and thermal conduction.

RELATED WORK

Among the numerous studies of combined free and forced convection the most relevant are the single phase flow studies of Shannon and Depew [2] and Cheng *et al.* [3]. The former experimentally studied combined free and forced convection for flow in a horizontal tube with uniform heat flux, and they successfully correlated their Nusselt number data with the dimensionless group $Ra_T^{1/4}/Nu_{Gz}$, where the Rayleigh number, Ra_T, is defined in terms of the temperature difference between the wall and the bulk fluid, $T_w - T_B$; that is, $Ra_T = g\beta(T_w - T_B)D^3/\alpha\nu$. Natural convection starts to manifest itself when $Ra_T^{1/4}/Nu_{Gz} = 2$. The enhancement of heat transfer by natural convection was found to be 250 per cent at $x/D \sim 700$, where D is the tube diameter.

By means of finite difference solutions of the appropriate governing equations of motion and energy Cheng *et al.* analyzed the buoyancy effects on laminar flow heat transfer in channels with various aspect ratios (width to channel height) and for uniform heat flux around the periphery of the heated duct. They presented solutions for the stream functions, isotherms and Nusselt numbers as functions of dimensionless axial distance. Cheng *et al.* wrote the Rayleigh number in terms of the equivalent diameter, D_e, of the channel and the heat flux, q_w; that is, $Ra_q = g\beta q_w D_e^4/\alpha k\nu$. For a circular tube Ra_T and Ra_q are related by $Ra_T = Ra_q/Nu$, so Shannon and Depew's criterion for the onset of natural convection may be written as $(Ra_q/Nu)^{1/4}/Nu_{Gz} = 2$.

Although the present study involves stratified gas–liquid flow and the aspect ratio of the liquid layer is essentially infinite, as we shall show, there are some striking similarities between the results of Shannon and Depew, Cheng *et al.* and those presented here.

GOVERNING EQUATIONS

The coordinates and a schematic diagram of the system are shown in Fig. 1. The liquid layer, assumed to be hydrodynamically fully developed at $x = 0$ and at uniform temperature T_0 in the region $x < 0$, flows under the influence of a small pressure gradient and the shear of a concurrently flowing gas phase. The heated section is maintained at constant heat flux, q_w.

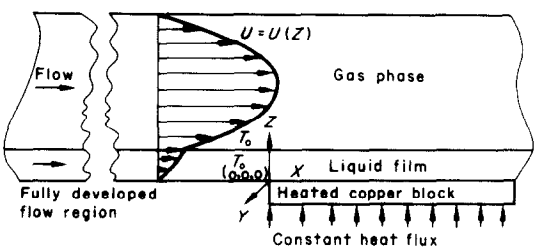

FIG. 1. The system under consideration.

Using the Boussinesq approximation for the liquid density and denoting undisturbed flow quantities by a bar, the equations of continuity, motion and energy become:

$$\frac{\partial}{\partial x}(\bar{U}+U)+\frac{\partial V}{\partial y}+\frac{\partial W}{\partial z}=0 \tag{1}$$

$$(\bar{U}+U)\frac{\partial}{\partial x}(\bar{U}+U)+V\frac{\partial}{\partial y}(\bar{U}+U)+W\frac{\partial}{\partial z}(\bar{U}+U) = -\frac{1}{\rho_o}\frac{\partial}{\partial x}(\bar{P}+P)+\nu\nabla^2(\bar{U}+U) \tag{2}$$

$$(\bar{U}+U)\frac{\partial V}{\partial x}+V\frac{\partial V}{\partial y}+W\frac{\partial V}{\partial z} = -\frac{1}{\rho_o}\frac{\partial}{\partial y}(\bar{P}+P)+\nu\nabla^2 \tag{3}$$

$$(\bar{U}+U)\frac{\partial W}{\partial x}+V\frac{\partial W}{\partial y}+W\frac{\partial W}{\partial z} = -\frac{1}{\rho_o}\frac{\partial}{\partial z}(\bar{P}+P)+\nu\nabla^2 W+g\beta(T-T_0) \tag{4}$$

$$(\bar{U}+U)\frac{\partial T}{\partial x}+V\frac{\partial T}{\partial y}+W\frac{\partial T}{\partial z}=\alpha\nabla^2 T \tag{5}$$

where ρ_o is the density at temperature T_0.

Now the undisturbed flow satisfies

$$\frac{1}{\rho_o}\frac{\partial \bar{P}}{\partial x} = \nu \frac{\partial^2 \bar{U}}{\partial z^2} \tag{6}$$

and

$$\frac{\partial \bar{U}}{\partial x} = 0. \tag{7}$$

To reduce equations (1)–(5) to nondimensional form we introduce the nondimensional variables

$$\xi = \frac{x}{\delta Re Pr}, \quad \eta = \frac{y}{\delta}, \quad \zeta = \frac{z}{\delta}, \quad u = \frac{U}{\bar{U}_m},$$

$$v = \frac{V\delta}{\alpha}, \quad w = \frac{W\delta}{\alpha}, \quad p = \frac{P\delta^2}{\mu\alpha}, \quad \theta = \frac{T-T_0}{q_w\delta/k},$$

$$Pr = \frac{\nu}{\alpha}, \quad Re = \frac{\bar{U}_m\delta}{\nu}, \quad Ra_q = \frac{g\beta q_w \delta^4}{\alpha k \nu}.$$

Substituting these variables in the governing equations and using equations (6) and (7) for the undisturbed flow, the governing equations become:

$$\frac{\partial u}{\partial \xi} + \frac{\partial v}{\partial \eta} + \frac{\partial w}{\partial \zeta} = 0 \tag{8}$$

$$\frac{1}{Pr}\left[(\bar{u}+u)\frac{\partial u}{\partial \xi} + v\frac{\partial u}{\partial \eta} + w\frac{\partial}{\partial \zeta}(\bar{u}+u)\right] = \frac{\partial^2 u}{\partial \eta^2} + \frac{\partial^2 u}{\partial \zeta^2} \tag{9}$$

$$\frac{1}{Pr}\left[(\bar{u}+u)\frac{\partial v}{\partial \xi} + v\frac{\partial v}{\partial \eta} + w\frac{\partial v}{\partial \zeta}\right] = -\frac{\partial p}{\partial \eta} + \frac{\partial^2 v}{\partial \eta^2} + \frac{\partial^2 v}{\partial \zeta^2} \tag{10}$$

$$\frac{1}{Pr}\left[(\bar{u}+u)\frac{\partial w}{\partial \xi} + v\frac{\partial w}{\partial \eta} + w\frac{\partial w}{\partial \zeta}\right] = -\frac{\partial p}{\partial \zeta} + \frac{\partial^2 w}{\partial \eta^2} + \frac{\partial^2 w}{\partial \zeta^2} - Ra_q\theta \tag{11}$$

$$(\bar{u}+u)\frac{\partial \theta}{\partial \xi} + v\frac{\partial \theta}{\partial \eta} + w\frac{\partial \theta}{\partial \zeta} = \frac{\partial^2 \theta}{\partial \eta^2} + \frac{\partial^2 \theta}{\partial \zeta^2}. \tag{12}$$

Since the Peclet number, $Pe = PrRe$, is large for the conditions of interest here we have neglected the axial conduction term, $(1/Pe^2)(\partial^2\theta/\partial\xi^2)$, in the energy equation and all other terms with coefficients, $1/Pe^2$, in the equations. Furthermore, as shown by Davis and Cooper [4], when the system is stable with respect to interfacial waves the interfacial shear force on the liquid film is large compared with the force associated with the pressure gradient, and equation (6) approximates to:

$$\frac{\partial^2 \bar{u}}{\partial \zeta^2} = 0. \tag{13}$$

Integrating equation (13) twice and applying the boundary conditions on the undisturbed flow

$$[\bar{u}(0) = 0,\ \bar{u}(1) = 2],$$

we find that the velocity distribution corresponds to Couette flow, $\bar{u} = 2\zeta$.

Thus, the undisturbed temperature distribution is the solution of the modified Graetz problem:

$$2\zeta\frac{\partial \theta}{\partial \xi} = \frac{\partial^2 \theta}{\partial \zeta^2}, \tag{14}$$

$$\theta(0,\zeta) = \theta(\xi,1) = 0, \qquad \frac{\partial \theta}{\partial \zeta}(\xi,0) = -1,$$

which as the solution [4]

$$\theta_{Gr}(\xi,\zeta) = 1 - \zeta + \sum_{n=1}^{\infty} A_n \zeta^{1/2} J_{-1/3}(\tfrac{2}{3}\lambda_n \zeta^{3/2}) \exp\left(-\frac{\lambda_n^2}{2}\xi\right), \tag{15}$$

where the Fourier coefficients, A_n, are obtained by applying the boundary condition at $\xi = 0$, using the orthogonality properties of

$$\zeta^{1/2} J_{-1/3}(\tfrac{2}{3}\lambda\zeta^{3/2}) \quad \text{for} \quad \lambda = \lambda_n, \lambda_m.$$

The Nusselt number for the undisturbed flow is given by:

$$Nu_{Gz} = \frac{q_w\delta}{k(T_w - T_B)} = \frac{1}{\theta_w - \theta_B} \tag{16}$$

where the dimensionless wall temperature is given by $\theta_w = \theta_{Gz}(\xi, 0)$, and the mixed mean temperature, θ_B, is calculated from:

$$\theta_B = 2\int_0^1 \zeta\theta_{Gz}(\xi,\zeta)\,d\zeta. \tag{17}$$

When the buoyant force is sufficient to destabilize the system, it is necessary to solve equations (8) through (12) to determine the temperature field and the heat-transfer characteristics of the system. Cheng *et al.* solved a similar set of equations for $Pr = \infty$ to obtain their results for a rectangular channel. It is not our purpose here to solve the governing equations for the particular geometry and boundary conditions of this problem, but to use the equations to identify the significant dimensionless groups that must be taken into account in the correlation of heat-transfer enhancement data. We shall define the enhancement factor, E, as

$$E = \frac{Nu - Nu_{Gz}}{Nu_{Gz}}, \tag{18}$$

where Nu is the Nusselt number for the combined free and forced convection heat transfer.

It is clear from the governing equations that Nu depends on the parameters Ra_q and Pr. It is the purpose of the experimental study to determine the functional relationship between Nu, Ra_q, Pr, Nu_{Gz}, and E and to study the nature of the instability and the resulting secondary flow that occurs.

EXPERIMENTS

The equipment is essentially the same as that used by Frisk and Davis. Air, supplied by a turbo compressor, was cooled and saturated in a spray chamber, passed through a plenum chamber and through a section containing tubes to straighten the flow, then flowed through a converging section, which served as a venturi, to measure the flow rate. The test section,

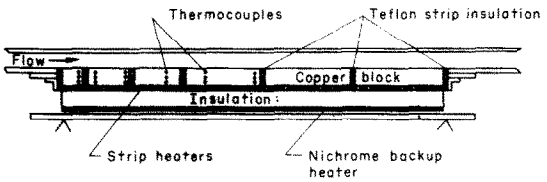

FIG. 2. The heat-transfer test section.

a 6·1 m long plexiglas wind tunnel 25 cm in width by 2·61 cm in height, was connected to the venturi by means of a flexible rubber section to minimize vibration. A metered (by rotameter) stream of water was introduced through perforations in the tunnel bottom near the air inlet. The heat-transfer section consisted of a 60·1 cm copper block inserted flush with the tunnel bottom. The upstream edge of the block was 4·9 m from the air inlet. The copper block was cut into 6 sections, as indicated in Fig. 2, and the sections were insulated from each other by 1·6 mm thick Teflon sheets. The purpose of the insulation is to eliminate the axial conduction in the block produced by variations in the surface temperature of the block due to heat transfer to the liquid film. The significant effect of the axial conduction in the copper block was critically examined by Davis and Gill [5]. Since axial conduction would be most pronounced near the upstream edge of the block, the sections were shortest near the leading edge, increasing in length as one proceeds downstream. Electrical strip heaters were installed beneath the copper block, each set of heaters being controlled by separate variable transformers. The electrical power supplied to each section was measured by using calibrated voltmeters and ammeters. For all the data reported in the present work, a constant heat flux was used. The energy supplied to the liquid film and the flow rates were adjusted such that the error in the energy balance (power input compared with the enthalpy increase of the liquid film) on the liquid film was within 5 per cent. Other measurements and details are discussed in [1].

FLOW VISUALIZATION

To independently measure the point of onset of natural convection (heat transfer data were one measure) and to examine the characteristics of the disturbed flow a dye injection flow visualization technique was used. A thin stream of dye was injected from a

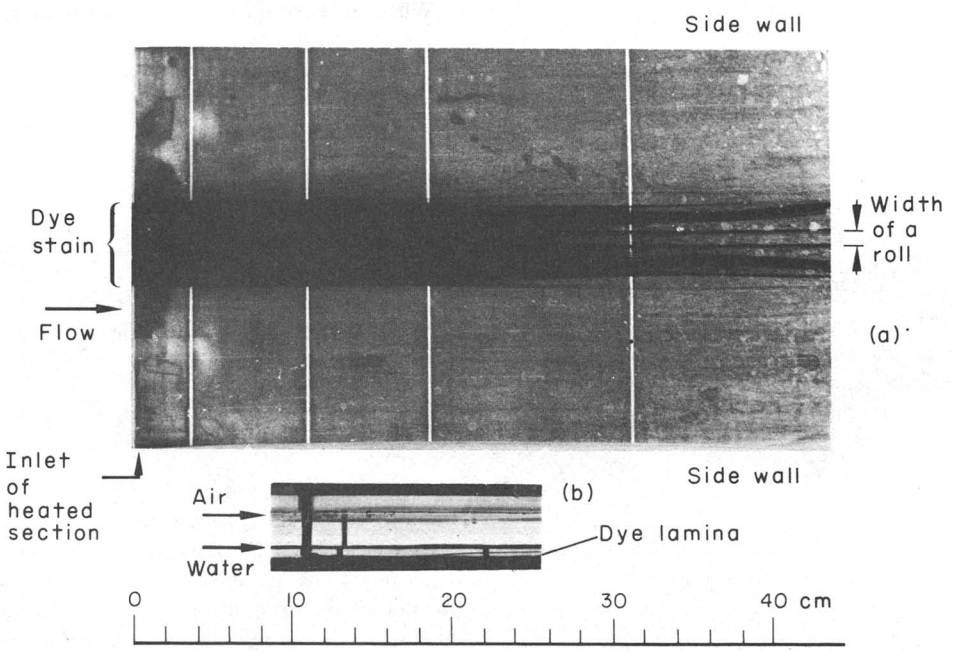

FIG. 3. Top and side views with flow visualization.

fine hyperdermic needle onto the bottom of the water-wind tunnel just upstream of the heat-transfer test section. The dye spread over a wide region as shown in Fig. 3(a), a top view of the heat-transfer section. The corresponding side view, Fig. 3(b), shows that the dye flows along the surface of the heated block until a point is reached at which natural convection causes the dye to move upward, off the bottom, as a thin lamina. Farther downstream the lamina becomes unstable, and the dye stream follows the longitudinal roll cells that develop. The top view shows the boundaries of some of the roll cells that develop. The width of a roll cell is indicated in the figure. An observer sees the spiral motion associated with the secondary flow in the downstream region.

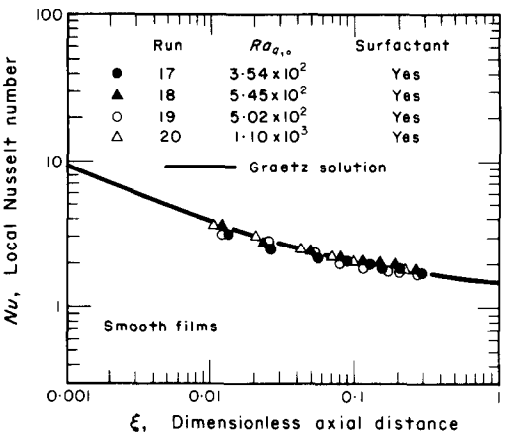

FIG. 4. Comparison of Nusselt numbers for undisturbed flow with the Graetz solution.

HEAT TRANSFER RESULTS

The experimental Nusselt numbers were obtained by measuring the heat flux, q_w, the film thickness, δ, and the local wall temperature, T_w. The mixed mean temperature T_B was obtained from measurements of the inlet temperature, T_0, the liquid flow rate and the heat input up to the axial position in question. The wall temperature was obtained by extrapolating the measured temperature profiles in the copper block. The flow parameters and other information for the experiments are summarized in Table 1.

For low Rayleigh numbers the flow is not disturbed by natural convection and the Nusselt numbers, shown in Fig. 4, are in good agreement with the solution presented as equations (15) and (16). For the runs corresponding to Fig. 4 trace amounts of a surfactant were added to the liquid phase to suppress interfacial waves, as discussed by Narasimhan and Davis [6]. There is no indication of surface tension driven instability caused by the introduction of a soluble surfactant.

To confirm that the Reynolds number of the liquid phase has no effect on the heat-transfer results (other than that included in the dimensionless distance, ξ) if the Rayleigh and Prandtl numbers are not varied when natural convection occurs, we carried out experiments at various liquid phase Reynolds numbers ($247 \leqslant Re \leqslant 467$) at essentially constant Ra_q and Pr.

Table 1. Summary of experimental parameters

Run No.	Natural convection	σ (dyne/cm)	T_0 (°K)	δ (cm)	q_w (J/m² s)	$Ra_{q,o}$	Re_o	$Re_{G,o}$	Pr_o
1	yes	—	300·4	0·620	$1·9 \times 10^4$	$7·42 \times 10^5$	540	2798	5·88
2	yes	—	304·3	0·635	$9·0 \times 10^3$	$4·13 \times 10^5$	416	1664	5·28
3	yes	—	300·2	0·592	$9·0 \times 10^3$	$2·92 \times 10^5$	436	1672	5·88
4	yes	—	300·3	0·511	$9·0 \times 10^3$	$1·62 \times 10^5$	369	1930	5·88
5	yes	—	300·2	0·508	$9·0 \times 10^3$	$1·58 \times 10^5$	310	1672	5·88
6	yes	—	299·9	0·493	$9·0 \times 10^3$	$1·41 \times 10^5$	247	1673	5·88
7	yes	—	300·2	0·282	$9·0 \times 10^3$	$1·51 \times 10^4$	83	3481	5·88
8	yes	—	300·1	0·564	$9·0 \times 10^3$	$2·41 \times 10^5$	411	2731	5·88
9	yes	—	300·5	0·511	$9·0 \times 10^3$	$1·62 \times 10^5$	280	1930	5·88
10	yes	—	300·3	0·450	$9·0 \times 10^3$	$9·76 \times 10^4$	165	1931	5·88
11	yes	—	299·1	0·321	$3·3 \times 10^3$	$9·10 \times 10^3$	81	4216	6·05
12	yes	—	291·2	0·213	$9·2 \times 10^3$	$4·33 \times 10^3$	104	2540	7·40
13	yes	—	291·9	0·206	$9·1 \times 10^3$	$3·80 \times 10^3$	106	2800	7·25
14	yes	—	290·4	0·203	$9·1 \times 10^3$	$3·46 \times 10^3$	102	2840	7·63
15	yes	59·74	300·3	0·500	$9·0 \times 10^3$	$1·49 \times 10^5$	467	4097	5·88
16	yes	55·51	300·6	0·353	$9·0 \times 10^3$	$3·70 \times 10^4$	226	4095	5·81
17	no	49·00	288·5	0·094	$2·1 \times 10^4$	$3·54 \times 10^2$	242	15 540	8·03
18	no	49·00	289·4	0·104	$2·1 \times 10^4$	$5·45 \times 10^2$	248	14 720	7·81
19	no	56·68	290·7	0·104	$1·9 \times 10^4$	$5·02 \times 10^2$	239	12 450	7·56
20	no	50·72	289·1	0·127	$1·9 \times 10^4$	$1·10 \times 10^3$	234	11 230	7·81

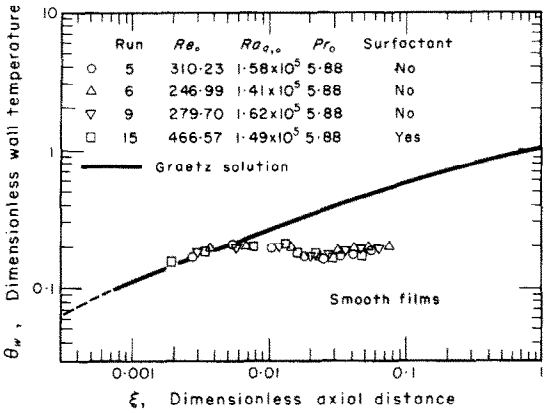

FIG. 5. The dimensionless wall temperature for combined free and forced convection for various liquid phase Reynolds numbers.

The results, plotted as θ_w vs ξ, are shown in Fig. 5. Also shown in the figure is the Graetz solution from equation (15). Note that at $\xi = 0{\cdot}005$ the results begin to deviate from the Graetz solution due to the onset of natural convection. The data for various Re are nearly indistinguishable.

The effects of varying the Rayleigh number for a fixed Prandtl number ($Pr = 5{\cdot}9$) are shown in Fig. 6. For small values of ξ, where the thermal boundary layer is thin, the experimental Nusselt numbers agree with the Graetz solution; but, in each case shown, natural convection begins at some axial position that depends on the Rayleigh number. For large Ra_q considerable heat-transfer enhancement occurs for large ξ. For the data presented here there are no apparent asymptotic Nusselt numbers. This is probably due to the fact that, with constant flux heating, a stable secondary flow does not occur. The longitudinal roll waves eventually become unstable and decay to a turbulent flow field.

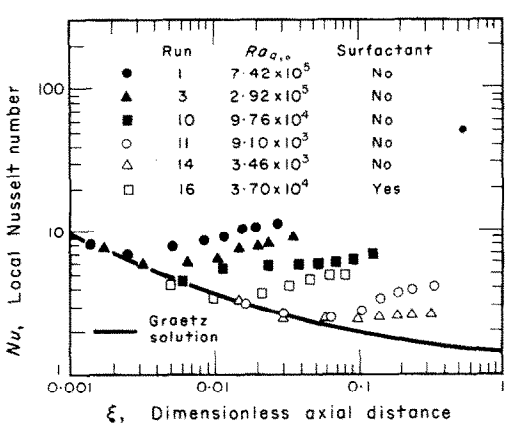

FIG. 6. The effect of the Rayleigh number on the onset of natural convection.

From the successful correlation by Shannon and Depew for flow in heated circular tubes we are led to examine the correlation of heat-transfer enhancement with the parameter $\phi \equiv (Ra_q/Nu)^{1/4}/Nu_{Gz}$. Using the definition of E from equation (18), we have plotted E as a function of ϕ for all of the data taken in these experiments. For $\phi < 2{\cdot}8$ stable laminar flow occurred; the scatter in that data is primarily due to the small temperature differences $(T_w - T_B)$ encountered. The scatter in the data for $\phi > 2{\cdot}8$ is not unreasonable, considering the accuracy of the data and the fact that the Prandtl number varied somewhat from run to run ($5{\cdot}28 < Pr < 8{\cdot}03$).

The data for the region $\phi > 2{\cdot}8$ are correlated by

$$E = 0{\cdot}94(\phi - 2{\cdot}8). \tag{19}$$

Note that the enhancement exceeds 300 per cent for $\phi \sim 6$. The data for runs in which surfactants were used show no significant differences from runs involving an uncontaminated interface. This fact supports the assumption that Marangoni instability is not involved here.

Figure 7 shows that the onset of natural convection is fairly sharply defined as occurring when $\phi = \phi_c = 2{\cdot}8$. At the onset of natural convection the Nusselt number, Nu, can still be represented by the Graetz solution; and, hence, we may write

$$\phi_c = (Ra_q)_c^{1/4}/(Nu_{Gz})^{5/4}. \tag{20}$$

Thus, the critical Rayleigh number, $(Ra_q)_c$, is given by

$$(Ra_q)_c = (2{\cdot}8)^4[\theta_{Gz}(\xi, 0) - \theta_B(\xi)]^{-5}, \tag{21}$$

using equations (20) and (16). Equation (21) is compared with data on the onset of natural convection in Fig. 8. The agreement with the results based on heat-transfer data is excellent, but the results based on the flow visualization studies consistently lie above

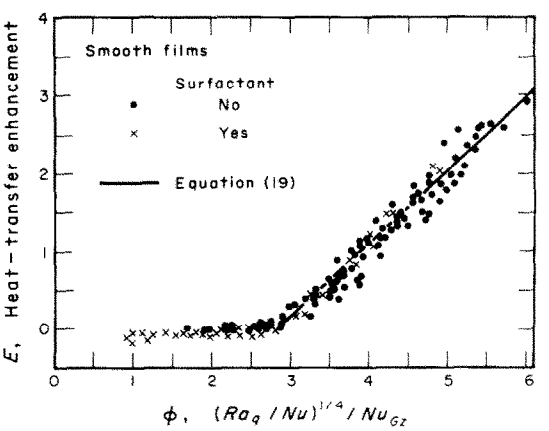

FIG. 7. The enhancement of heat transfer associated with combined free and forced convection.

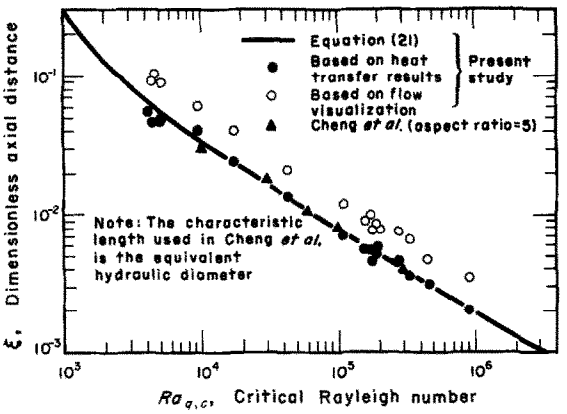

FIG. 8. The position of the onset of natural convection as a function of the Rayleigh number.

and parallel to those for heat transfer. Since the physical properties of the dye stream are somewhat different than the properties of the water, it is likely that the disagreement is attributable to physical property differences. For any particular run it could be observed that the dye stream remained in contact with the heat transfer surface for a short distance beyond where the heat transfer data indicated the onset of natural convection.

Also plotted on Fig. 8 are the results of the analysis of Cheng *et al.* for the onset of natural convection in a rectangular duct with an aspect ratio of 5, the largest aspect ratio they considered. Their results are in excellent agreement with our data. This is a somewhat surprising result considering the different flow configurations involved, but it suggests that the mode of instability is similar in the two cases. Furthermore, the agreement suggests that the Prandtl number effect is not great for $Pr > 5$.

It should be pointed out that two-dimensional ripples at the gas–liquid interface have no effect on the onset of natural convection, which indicates that the disturbances associated with such surface waves do not penetrate significantly into the liquid layer to disturb the developing thermal boundary layer.

CONCLUSIONS

1. Heat-transfer enhancement associated with combined free and forced convection in the liquid phase for gas–liquid stratified flow is well correlated with the parameter $\phi = (Ra_q/Nu)^{1/4}/Nu_{Gz}$.

2. Heat-transfer data for undisturbed Couette flow of the liquid phase are in excellent agreement with a Graetz-like solution.

3. For the range of Prandtl numbers considered ($5 < Pr < 8$), the onset of natural convection is $\phi = 2{\cdot}8$, which compares with the value $\phi = 2{\cdot}0$ for available data in horizontal circular tubes, and is in good agreement with an available theoretical analysis for rectangular ducts.

4. The initial instability of the laminar flow is followed by the formation of longitudinal rolls.

Acknowledgement—The authors are grateful to the American Institute of Chemical Engineers-Design Institute for Multiphase Processing for the support of their research in two-phase flow heat transfer and to the National Science Foundation for Grant GK-41270.

REFERENCES

1. D. P. Frisk and E. J. Davis, The enhancement of heat transfer by waves in stratified gas–liquid flow, *Int. J. Heat Mass Transfer* **15**, 1537–1552 (1972).
2. R. L. Shannon and C. A. Depew, Combined free and forced laminar convection in a horizontal tube with uniform heat flux, *J. Heat Transfer* **90**, 353–357 (1968).
3. K. C. Cheng, S. W. Hong and G. J. Hwang, Buoyancy effects on laminar heat transfer in the thermal entrance region of horizontal rectangular channels with uniform wall heat flux for large Prandtl number fluid, *Int. J. Heat Mass Transfer* **15**, 1819–1836 (1972).
4. E. J. Davis and T. J. Cooper, Thermal entrance effects in stratified gas–liquid flow: experimental investigation, *Chem. Engng Sci.* **24**, 509–520 (1969).
5. E. J. Davis and W. N. Gill, The effect of axial conduction in the wall on heat transfer with laminar flow, *Int. J. Heat Mass Transfer* **13**, 459–470 (1970).
6. T. V. Narasimhan and E. J. Davis, Surface waves and surfactant effects in horizontal stratified gas–liquid flow, *IEC Fundamentals* **11**, 490–497 (1972).

CONVECTION NATURELLE DANS UN ECOULEMENT STRATIFIE GAZ-LIQUIDE ET ACCROISSEMENT DU TRANSFERT THERMIQUE

Résumé—On présente des résultats expérimentaux sur le transfert thermique et sur la visualisation qui montrent l'organisation de la convection naturelle dans une couche liquide d'un écoulement gaz–liquide horizontal stratifié, chauffé par la base selon un échelon de flux thermique pariétal. On montre que le nombre de Nusselt Nu, pour la convection mixte, est fonction du nombre de Rayleigh Ra_q et de la distance adimensionnelle à l'axe ξ. L'accroissement de transfert thermique par rapport à l'écoulement non perturbé (problème de Graetz) est fonction du paramètre adimensionnel $\phi = (Ra_q/Nu)^{1/4}/Nu_{Gz}$. L'organisation de la convection naturelle prend place à $\phi = 2{,}8$ pour le domaine àtroit des nombres de Prandtl étudiés ($5 < Pr < 8$), ce qui est en bon accord avec une analyse théorique de la convection naturelle dans les conduites à section droite rectangulaire.

DER BEGINN DER NATÜRLICHEN KONVEKTION UND IHRE STEIGERUNG DURCH DIE WÄRMEÜBERTRAGUNG IN GESCHICHTETEN GAS-FLÜSSIGKEITS-STRÖMUNGEN

Zusammenfassung—Es werden Ergebnisse von Wärmeübertragungsversuchen und Studien über sichtbar gemachte Strömungen vorgelegt, welche den Beginn der natürlichen Konvektion in der flüssigen Phase einer von unten beheizten, waagerecht geschichteten Gas-Flüssigkeits-Strömung durch eine plötzliche Änderung des Wärmeflusses an der Wand anzeigen. Es wird gezeigt, daß die Nusselt-Zahlen Nu für zusammengesetzte freie und erzwungene Konvektion Funktionen der Rayleigh-Zahl Ra_q und des dimensionslosen axialen Abstands ξ sind. Der besondere Einfluß der Wärmeübertragung gegenüber dem der ungestörten Strömung (ein Graetz-Problem) wird durch den dimensionslosen Parameter $\phi = (Ra_q/Nu)^{1/4}/Nu_{Gz}$ gut wiedergegeben.

ВОЗНИКНОВЕНИЕ ЕСТЕСТВЕННОЙ КОНВЕКЦИИ И ИНТЕНСИФИКАЦИЯ ТЕПЛООБМЕНА В СЛОИСТОМ ГАЗО-ЖИДКОСТНОМ ПОТОКЕ

Аннотация — Представлены экспериментальные результаты по теплообмену и визуализации потока, показывающие возникновение естественной конвекции в жидкостной прослойке горизонтально слоистого газо-жидкостного нагреваемого снизу потока при ступенчатом изменении теплового потока на стенке. Показано, что числа Нуссельта Nu при совместной свободной и вынужденной конвекции зависят от числа Релея, Ra_q, и безразмерного расстояния по оси ξ. С помощью безразмерного параметра $\phi = (Ra_q/Nu)^{1/4}/Nu_{GZ}$ обобщены данные по интенсификации теплообмена по сравнению с теплообменом невозмущенного потока (задача Гретца). Естественная конвекция возникает при $\phi = 2{,}8$ в ограниченном диапазоне изменения чисел Прандтля ($5 < Pr < 8$), что хорошо согласуется с имеющимися для каналов прямоугольного сечения теоретическими данными по возникновению естественной конвекции.